

Spherulites as in-situ recorders of thermal history in lava flows

Kenneth S. Befus¹, James Watkins², James E. Gardner¹, Dominique Richard³, Kevin M. Befus¹, Nathan R. Miller¹, and Donald B. Dingwell³

¹Jackson School of Geosciences, The University of Texas at Austin, Austin, Texas 78712, USA

²Department of Geological Sciences, University of Oregon, Eugene, Oregon 97403, USA

³Department of Earth and Environmental Sciences, Ludwig Maximilian University of Munich, Theresienstrasse 41/III, 80333 Munich, Germany

ABSTRACT

Spherulites in rhyolitic obsidian provide a record of the thermal history of their host lava during the interval of spherulite growth. We use trace element concentration profiles across spherulites and into the obsidian host from Yellowstone National Park (USA) to reconstruct the conditions that existed during spherulite formation. The measured transects reveal three behaviors: expulsion of the most diffusively mobile elements from spherulites with no concentration gradients in the surrounding glass (type 1); enrichment of slower-diffusing elements around spherulites, with concentration gradients extending outward into the glass (type 2); and complete entrapment of the slowest-diffusing elements by the spherulite (type 3). We compare the concentration profiles, measured by laser ablation–inductively coupled plasma–mass spectrometry and Fourier transform infrared spectroscopy, to the output of a spherulite growth model that incorporates known diffusion parameters, the temperature interval of spherulite growth, the cooling rate of the lava, and data on the temporal evolution of spherulite radius. Our results constrain spherulite nucleation to the temperature interval 700–550 °C and spherulite growth to 700–400 °C in a portion of lava that cooled at $10^{-5.2 \pm 0.3}$ °C s⁻¹, which matches an independent experimental estimate of $10^{-5.3}$ °C s⁻¹ measured using differential scanning calorimetry. Maximum spherulite growth rates at nucleation are on the order of 1 μm hr⁻¹ and are inferred to decrease exponentially with time. Hence, spherulites may serve as valuable in-situ recorders of the thermal history of lava flows.

INTRODUCTION

The striking appearance of millimeter- to centimeter-scale light-colored spherulites in dark obsidian outcrops became a subject of scientific inquiry more than a century ago (Cross, 1891). Studies in the intervening years have documented occurrences of spherulites, their field distributions, and their textural characteristics (Ewart, 1971; Manley and Fink, 1987; Tuffen and Castro, 2009). Beyond their historical role as a curiosity to petrologists as well as rock collectors, spherulites have recently been recognized for their scientific value as recorders of past magmatic conditions. The distributions of trace elements within and around spherulites appear to contain information on crystallization rates, redox reactions, and the thermal history of the host lava (Castro et al., 2008, 2009; Watkins et al., 2009; Gardner et al., 2012; von Aulock et al., 2013).

Spherulites in rhyolitic lavas are spherical to ellipsoidal bodies of radiating, intergrown crystals, typically feldspar and quartz, that form by rapid crystallization of lava in response to significant cooling (Lofgren, 1971a, 1971b; Fenn, 1977; Swanson, 1977). As spherulites grow, incompatible constituents are expelled into the surrounding melt or glass, creating enrichments of those elements along the spherulite–host boundary (Castro et al., 2008; Watkins et al., 2009; Gardner et al., 2012). With time, the expelled constituents diffuse away from the spherulite and into the surrounding host at tem-

perature-dependent rates. The process of expulsion and diffusion of the incompatible elements generates element-specific concentration profiles, the shapes of which depend on spherulite growth rate, element diffusivity, and the cooling rate of the host lava (Gardner et al., 2012).

If two of the above quantities can be estimated independently, then it should be possible to determine the unknown third quantity by direct inference from measurements on spherulite-bearing glasses. Here, we measure concentration gradients around 19 individual spherulites and use published diffusion parameters to construct a numerical model for spherulite growth accompanied by outward diffusion of incompatible elements. We use differential scanning calorimetry (DSC) to independently determine the cooling rate of the sample investigated. With this information we construct model fits to measured diffusion profiles around spherulites of varying sizes to constrain spherulite growth through time. The result is a set of self-consistent physical parameters for spherulite growth and lava cooling. Insofar as the inferred spherulite growth law is generally applicable, we propose that spherulites act as in-situ recorders of the thermal history of spherulite-bearing glasses and welcome future tests of this proposal.

GEOLOGIC SETTING AND SAMPLE SELECTION

A hand sample of spherulite-bearing obsidian was collected from the Pitchstone Plateau lava

flow, a 70 km³ high-silica rhyolitic obsidian lava that traveled up to 16 km away from its vent, which erupted effusively at 79 ± 10 ka within Yellowstone caldera (western United States; see the GSA Data Repository¹; Christiansen et al., 2007). The sample was collected as a single, 2 kg block from an in-situ outcrop of relatively non-vesicular obsidian on the erosional surface of the flow near the eastern flow front, where the flow remains at least 180 m thick (sampling locality: 44.247°N, 110.680°W).

Spherulites compose a few percent of the obsidian sample by volume, and occur as 1–10 mm, near-spherical ellipsoids (Fig. 1A). Individual spherulites are distributed randomly throughout the sample, separated by tens of millimeters, with some clusters of two to four spherulites that impinge upon one another. All spherulites are composed of elongate crystals of alkali feldspar ($\text{Or}_{34 \pm 6}\text{Ab}_{64 \pm 6}\text{An}_{2 \pm 1}$) and quartz that radiate outward from a centralized nucleation site. Minor phases include equidimensional magnetite and randomly oriented, irregularly shaped voids that most likely represent vesicles. Quartz and alkali feldspar crystals are both longer and wider near the center of the spherulites. The ratio of alkali feldspar to quartz increases gradually outwards from the spherulite core, from near equal proportions near the center to ~60% alkali feldspar approaching the margin. The outermost ~100 μm is more porous and composed solely of radiating alkali feldspar crystals and void space. Pockets of glass trapped within the spherulites, documented in other studies (e.g., Castro et al., 2008), were not observed.

The spherulites are hosted within a high-silica rhyolitic glass (76 wt% SiO₂) that contains 5–10 vol% phenocrysts, 95% of which are sanidine and quartz, with the other 5% being magnetite, clinopyroxene, and fayalite. The glassy groundmass contains magnetite and clinopyroxene microlites, which define diffuse flow bands. Spherulites overprint those flow-induced textures, as evidenced by undeflected flow bands that can be traced from the matrix glass through the spherulites.

¹GSA Data Repository item 2015227, descriptions of analytical techniques, modeling parameters, and uncertainties, is available online at www.geosociety.org/pubs/ft2015.htm, or on request from editing@geosociety.org or Documents Secretary, GSA, P.O. Box 9140, Boulder, CO 80301, USA.

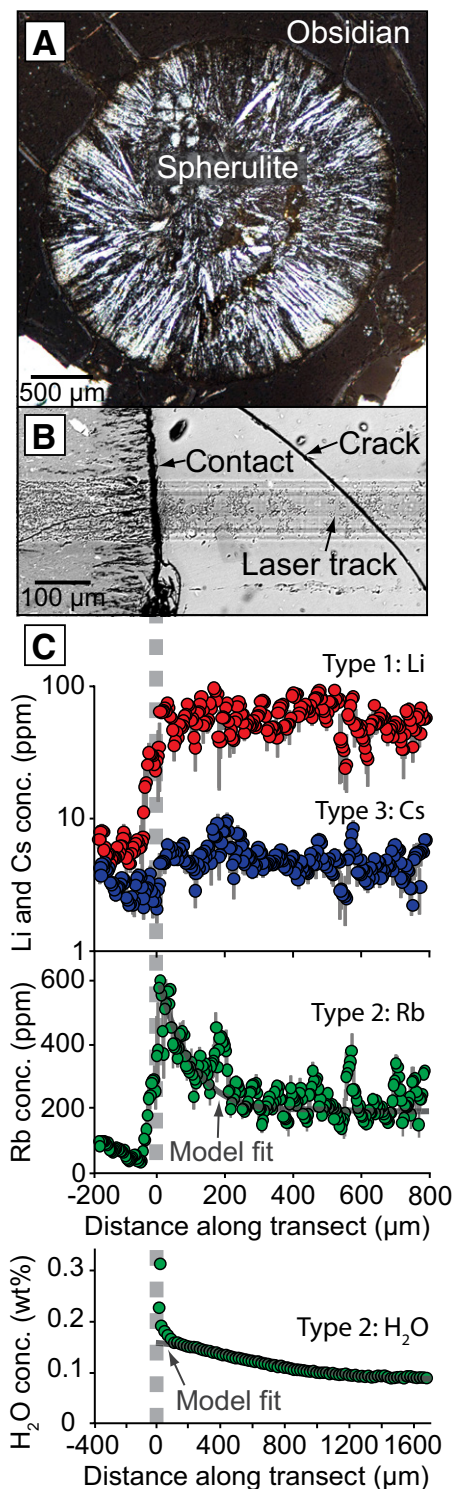


Figure 1. A: Photomicrograph (crossed polars) of spherulite composed of radiating crystals of quartz and feldspar hosted in dense obsidian glass. B: Backscattered image of spherulite-matrix contact crossed by laser ablation track. C: Examples of type 1 (Li, in red), type 2 (Rb and H₂O, in green), and type 3 (Cs, in blue) profiles (conc.—concentration). Spherulite-matrix boundary occurs at 0 μm, and is marked with dashed gray line. Data are from spherulite Yell-24-13 (2050 μm diameter). Error bars shown by gray bars where larger than symbol size.

CONCENTRATION PROFILES AROUND SPHERULITES

Trace element and H₂O concentration profiles were measured across the spherulite-glass interface by laser ablation–inductively coupled plasma–mass spectrometry and Fourier Transform infrared spectroscopy, respectively (Fig. 1B; see the Data Repository). Overall, three types of behavior have been recognized (cf. Gardner et al., 2012) (Fig. 1C). The fastest-diffusing elements (Li and K) follow “type 1” behavior, exhibiting uniformly low concentrations in the spherulite and uniformly higher concentrations in the glass. Such profiles are interpreted to result from rapid diffusion away from the spherulite during spherulite growth. A group of slower-diffusing components (Rb and H₂O) follow “type 2” behavior, exhibiting enrichments in the glass surrounding spherulites, with concentration decreasing with distance from the boundary. Such profiles are thought to result from trace elements diffusing at rates comparable to that of spherulite growth. The slowest-diffusing incompatible elements (B, Cs, Mn, Mg, Pb, Ba, Sr, and Sc) follow “type 3” behavior, whereby the elements diffuse far slower than spherulites grow, such that concentrations are unchanged across the spherulite-glass boundary and the elements are trapped in the growing spherulite. Here it is important to clarify that all H₂O profiles are modified near the spherulite-matrix boundary by a steep increase in concentration caused by secondary hydration, and thus the steep increases are disregarded in our treatment (see the Data Repository).

SPHERULITE GROWTH DURING LAVA COOLING

We employ a numerical crystal growth and diffusion model that uses known temperature-dependent, element-specific diffusion coefficients to generate model concentration profiles (see the Data Repository). At each time step in the model, the spherulite boundary moves according to the specified temperature-dependent growth rate and a constant fraction of each trace element is expelled into the glass. Whereas type 1 and type 3 profiles provide constraints on the temperature window of spherulite growth, we focus the discussion on the type 2 profiles of Rb and H₂O, because these offer the most restrictive constraints on the conditions of spherulite formation.

In the spherulite growth model, the shape of the type 2 concentration profiles depends on (1) the temperature window over which spherulites nucleate and grow, (2) the temperature-time path of the spherulite, i.e., the cooling rate of the lava flow, and (3) the temperature-dependent growth rate (Gardner et al., 2012). The shapes of the measured and modeled diffusion profiles can be quantified in terms of two parameters: (1) the concentration enrichment at the spheru-

lite boundary, and (2) the propagation distance (Table DR1 in the Data Repository). Enrichment (ϵ) is defined as the concentration of an element in the glass at the spherulite-glass boundary, normalized to its concentration far from the spherulite, and then converted to a percentage. In the model, spherulite growth rates strongly control ϵ , with faster growth leading to greater ϵ . For the propagation distance (P_{Δ}), we use a different metric than the commonly used e -fold distance for describing the shape of diffusion profiles. The reason for doing so is to be able to plot “diffusion profile shape” as ϵ/P_{Δ} on the y -axis versus spherulite radius on the x -axis in order to compare model to data from all spherulites simultaneously. If one were to use the e -fold distance (distance at which concentration decreases by a factor of e from the spherulite boundary), the ratio of enrichment to diffusion distance would be a non-unique description of diffusion profile shape. For the measured profiles, we calculate P_{Δ} as the distance from the spherulite margin that the elemental concentration exceeds by two standard deviations that measured in the glass host matrix. For the model profiles, P_{Δ} is the distance from the spherulite margin where the concentration first exceeds the background level by a set percentage. To establish model uncertainties in P_{Δ} , we use $12\% \pm 6\%$ and $5\% \pm 3\%$ for Rb and H₂O, respectively, as those values encompass the full range of standard deviations observed in the natural data. In the model, P_{Δ} increases mainly with slower cooling, faster growth, and growth at higher temperatures.

The first step in modeling spherulite growth is to specify how growth rate varies with temperature. In the absence of a general theory, we have investigated models that invoke constant, linearly decreasing, and exponentially decreasing radial growth laws (see the Data Repository). Both the constant radial and the linearly decreasing radial growth laws can be ruled out on the basis that they generate profiles with ϵ values much greater than those observed (Gardner et al., 2012). Our preference for the exponentially decreasing radial growth model stems from several factors: (1) it produces reasonable values of ϵ ; (2) it reproduces the positive correlations between ϵ , P_{Δ} , and spherulite size for both Rb and H₂O that are observed; and (3) it ultimately yields reasonable cooling rates for the host lava. Furthermore, this growth law is qualitatively consistent with the observation that crystal sizes decrease from core to rim. We therefore adopt the exponentially decreasing radial growth law as the best available description of the temperature dependence of spherulite growth.

With a specified growth law and measured diffusivities, the type 2 model profiles depend on the nucleation temperature, the temperature-dependent growth rate (note that growth rates are set to specific values at nucleation and

allowed to decrease following exponentially decreasing radial growth from that temperature), and the cooling rate of the host lava. We consider a broad parameter space of temperature (800–400 °C), growth rate (0.01–100 $\mu\text{m hr}^{-1}$), and cooling rate (10^{-3} to 10^{-7} $^{\circ}\text{C s}^{-1}$). In order to simultaneously match both Rb and H_2O , we find that nucleation temperatures must be roughly 625 ± 75 °C and that the cooling rate must be on the order of 10^{-5} $^{\circ}\text{C s}^{-1}$. We show the influence of varying the cooling rate and growth rate in Figures 2A and 2B, which are constructed by simulating spherulite growth and expulsion of Rb or H_2O at a fixed nucleation temperature of 600 °C. Figure 2A also shows the influence of varying the nucleation temperature. The cooling rate and growth rate curves that bracket the data provide a first-order estimate of the range of conditions over which the spherulites might have grown, provided that the assumptions built into the model are reasonably valid. Rb concentration data indicate that spherulites grew at 1.2 ± 0.6 $\mu\text{m hr}^{-1}$ while the lava cooled at $10^{-5.1 \pm 0.2}$ $^{\circ}\text{C s}^{-1}$ (Fig. 2A). H_2O data indicate that spherulites grew at 0.6 ± 0.3 $\mu\text{m hr}^{-1}$ while the lava cooled at $10^{-5.4 \pm 0.2}$ $^{\circ}\text{C s}^{-1}$ (Fig. 2B). The uncertainties are estimates based on a detailed assessment of Figure 2; see the Data Repository for further treatment of model uncertainties.

As a test of the model results, and to further constrain the conditions of spherulite growth, we determined the cooling rate of the obsidian sample via relaxation geospeedometry using DSC measurements (see the Data Repository). This method allows the cooling rate of a pristine glass sample to be inferred from the hysteresis exhibited in the heat capacity versus temperature curve obtained upon heating the natural glass across the glass transition.

The results yield a cooling rate of $10^{-5.3}$ $^{\circ}\text{C s}^{-1}$ across the glass transition temperature interval, with an uncertainty of +0.2 log units and –0.5 log units. Although this cooling rate is only representative of the sample’s thermal history at the crossing of the glass transition temperature, the value should closely approximate the slope of the temperature-time curve for a conductively cooled lava over the majority of its cooling (Manley, 1992).

Adopting the cooling rate of $10^{-5.3}$ $^{\circ}\text{C s}^{-1}$ from relaxation geospeedometry as the true cooling rate, we perform a similar analysis as above, treating instead growth rate and nucleation temperature as unknowns (Fig. 2C). Model results replicate Rb data using growth rates of ~ 0.4 $\mu\text{m hr}^{-1}$ (at 600 °C), whereas the model curves replicate H_2O data using growth rates of ~ 0.3 $\mu\text{m hr}^{-1}$ (at 600 °C). Note that these growth rate estimates are slightly slower than would be inferred from the earlier analysis (Figs. 2A and 2B), because the nucleation temperatures here are generally hotter than 600 °C. The two sets of data yield a nucleation temperature window of ~ 75 °C, with the H_2O data suggesting somewhat hotter nucleation temperatures than the Rb data. Although the two data sets should ideally yield the same growth rates and nucleation temperatures, we consider these values to be in reasonably good agreement given the many assumptions and uncertainties in the idealized spherulite growth and diffusion models.

To summarize, the form of the measured concentration gradients indicates that the spherulites grew with an exponentially decreasing radial growth style over a temperature window from ~ 700 °C to 400 °C. We interpret the range in spherulite sizes as a consequence of larger spherulites nucleating at hotter temperatures

than smaller spherulites. Spherulite growth and diffusion modeling of type 2 compositional profiles suggests a time-integrated cooling rate of $10^{-5.2 \pm 0.3}$ $^{\circ}\text{C s}^{-1}$ for the host lava during spherulite growth between 700 and 400 °C. That estimate, based only on the temperature range and style of spherulite growth, agrees with the cooling rate of $10^{-5.3}$ $^{\circ}\text{C s}^{-1}$ measured by relaxation geospeedometry at the glass transition. Consequently, we propose that spherulites act as in-situ recorders of thermal history and can therefore be used to explore both the cooling and crystallization of lava.

SPHERULITE GEOSPEEDOMETRY

To assess the viability of the modeling of concentration gradients around spherulites in relation to lava cooling and crystallization kinetics, we compare our results with experimental constraints on spherulite formation. Past experimental studies have examined how felsic minerals crystallize from melt in response to variable degrees of undercooling (Fenn, 1977; Swanson, 1977; Baker and Freda, 2001; Castro et al., 2009). Spherulites were the stable form in experiments that experienced large undercoolings ranging from 100 to 400 °C. The liquidus temperature of the Pitchstone Plateau lava with 0.1 wt% H_2O is estimated to be ~ 1000 °C using Rhyolite-MELTS software (Gualda et al., 2012). If true, then our estimated spherulite nucleation temperatures of ~ 600 –700 °C are equivalent to undercoolings of 300–400 °C, values similar to those determined in comparable experiments. Furthermore, quartz and alkali feldspar were experimentally estimated to grow at rates of 0.1–6 $\mu\text{m hr}^{-1}$, which are largely consistent with our estimates (Swanson, 1977; Baker and Freda, 2001; Castro et al., 2009).

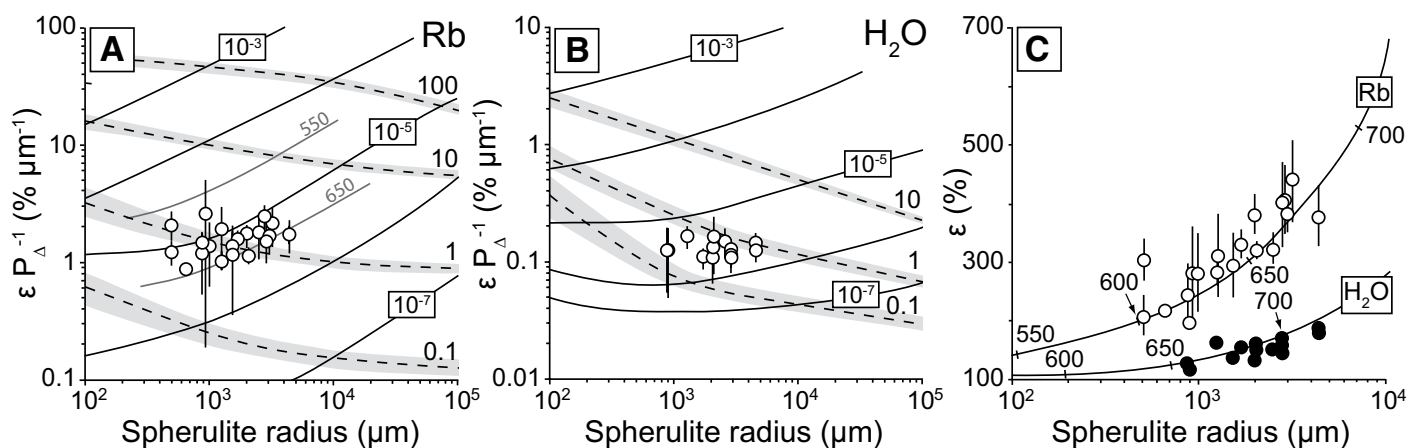


Figure 2. A,B: Ratio of ϵ (enrichment) to P_A (propagation distance) for Rb (A) and H_2O (B) as function of spherulite radius during exponentially decreasing growth. Solid black curves show lava cooling rates in $^{\circ}\text{C s}^{-1}$. Dashed curves are spherulite growth rates in $\mu\text{m hr}^{-1}$; gray fields represent model uncertainty. Model results were generated assuming nucleation temperature of 600 °C at the specified growth and cooling rates. In A labeled 550 and 650 show effect of changing nucleation temperature (in °C) on model results for 10^{-5} $^{\circ}\text{C s}^{-1}$. C: Model variations of ϵ as function of spherulite radius for exponentially decreasing radial growth. Assuming cooling rate of $10^{-5.3}$ $^{\circ}\text{C s}^{-1}$, data are duplicated when growth rates are set to 0.4 $\mu\text{m hr}^{-1}$ and 0.3 $\mu\text{m hr}^{-1}$ for Rb and H_2O , respectively, at 600 °C, which was then allowed to vary proportionally as function of nucleation temperature (tick marks in °C). Rb and H_2O data are shown as white and black circles, respectively; black lines represent error bars where larger than symbol size.

The cooling rate estimates determined independently from both techniques described herein can be interpreted to provide a first-order constraint on the longevity of a large-volume prehistoric lava. The duration over which lava flows are mobile is, amongst other factors, controlled by how fast lavas cool. That in turn is largely determined by how efficiently the upper crust and basal breccia can insulate the interior of the flow from heat loss (Walker et al., 1973). Before the rhyolitic effusion at Cordón Caulle volcano in Chile in A.D. 2011–2012 provided direct observations (Tuffen et al., 2013), effusive rhyolitic eruptions had been largely absent from the historic record, thus restricting our understanding of lava flow emplacement to studies of ancient eruptions (e.g., Fink, 1983; Castro and Cashman, 1999).

To illustrate a potential application of this technique, we extrapolate our results from spherulite geospeedometry to understand the emplacement of the host Pitchstone Plateau lava. If we conservatively assign the eruption temperature of Pitchstone Plateau to 750–800 °C (Vazquez et al., 2009) and assume the flow cooled at a rate of $10^{-5.3}$ °C s⁻¹ until it reached the glass transition temperature of 600–670 °C, then Pitchstone Plateau was emplaced in an absolute minimum of 230–460 days. Because our sample was collected near the surface of the flow, then it is likely that more thermally insulated interior portions remained mobile for much longer. Further, using that estimate as a minimum suggests that the flow front advanced at rates less than 70 m day⁻¹. Interestingly, the much smaller Cordón Caulle lava advanced at 1–4 m day⁻¹ (Tuffen et al., 2013). Although such estimates add to our ability to extract information on lava cooling, extrapolations of lava cooling rate must be considered with caution and analyzed with proper geologic context if applied to lava spreading. The veracity of these estimates now awaits testing in environments where active flows cease and the products can be sampled for analysis.

ACKNOWLEDGMENTS

Careful reviews by Eric Christiansen, Hugh Tuffen, and anonymous reviewers greatly improved this manuscript. This research was made possible by a grant from the National Science Foundation to Gardner

(grant EAR-1049829) and a National Park Service research permit (YELL-05678).

REFERENCES CITED

- Baker, D.R., and Freda, C., 2001, Eutectic crystallization in the undercooled Orthoclase-Quartz-H₂O system: Experiments and simulations: *European Journal of Mineralogy*, v. 13, p. 453–466, doi:10.1127/0935-1221/2001/0013-0453.
- Castro, J., and Cashman, K.V., 1999, Constraints on rheology of obsidian lavas based on mesoscopic folds: *Journal of Structural Geology*, v. 21, p. 807–819, doi:10.1016/S0191-8141(99)00070-X.
- Castro, J.M., Beck, P., and Tuffen, H., 2008, Timescales of spherulite crystallization in obsidian inferred from water concentration profiles: *The American Mineralogist*, v. 93, p. 1816–1822, doi:10.2138/am.2008.2904.
- Castro, J.M., Cottrell, E., Tuffen, H., Logan, A.V., and Kelley, K.A., 2009, Spherulite crystallization induces Fe-redox redistribution in silicic melt: *Chemical Geology*, v. 268, p. 272–280, doi:10.1016/j.chemgeo.2009.09.006.
- Christiansen, R.L., Lowenstern, J.B., Smith, R.B., Heasler, H., Morgan, L.A., Nathenson, M., Mastin, L.G., Muffler, L.J.P., and Robinson, J.E., 2007, Preliminary assessment of volcanic and hydrothermal hazards in Yellowstone National Park and vicinity: U.S. Geological Survey Open-File Report 2007-1071, 98 p.
- Cross, W., 1891, Constitution and origin of spherulites in acid eruptive rocks: *Bulletin of the Philosophical Society of Washington*, v. 11, p. 411–449.
- Ewart, A., 1971, Chemical changes accompanying spherulitic crystallization in rhyolitic lavas, Central Volcanic Region, New Zealand: *Mineralogical Magazine*, v. 38, p. 424–434, doi:10.1180/minmag.1971.038.296.04.
- Fenn, P.M., 1977, The nucleation and growth of alkali feldspars from hydrous melts: *Canadian Mineralogist*, v. 15, p. 135–161.
- Fink, J.H., 1983, Structure and emplacement of a rhyolitic obsidian flow: Little Glass Mountain, Medicine Lake Highland, northern California: *Geological Society of America Bulletin*, v. 94, p. 362–380, doi:10.1130/0016-7606(1983)94<362:SAEOAR>2.0.CO;2.
- Gardner, J.E., Befus, K.S., Watkins, J., Hesse, M., and Miller, N., 2012, Compositional gradients surrounding spherulites in obsidian and their relationship to spherulite growth and lava cooling: *Bulletin of Volcanology*, v. 74, p. 1865–1879, doi:10.1007/s00445-012-0642-9.
- Gualda, G.A.R., Ghiorsio, M.S., Lemons, R.V., and Carley, T.L., 2012, Rhyolite-MELTS: A modified calibration of MELTS optimized for silica-rich, fluid-bearing magmatic systems: *Journal of Petrology*, v. 53, p. 875–890, doi:10.1093/ptrology/egr080.
- Lofgren, G., 1971a, Experimentally produced devitrification textures in natural rhyolitic glass: *Geological Society of America Bulletin*, v. 82, p. 111–124, doi:10.1130/0016-7606(1971)82[111:EPDTIN]2.0.CO;2.
- Lofgren, G., 1971b, Spherulitic textures in glassy and crystalline rocks: *Journal of Geophysical Research*, v. 76, p. 5635–5648, doi:10.1029/JB076i023p05635.
- Manley, C.R., 1992, Extended cooling and viscous flow of large, hot rhyolite lavas: Implications of numerical modeling results: *Journal of Volcanology and Geothermal Research*, v. 53, p. 27–46, doi:10.1016/0377-0273(92)90072-L.
- Manley, C.R., and Fink, J.H., 1987, Internal textures of rhyolite flows as revealed by research drilling: *Geology*, v. 15, p. 549–552, doi:10.1130/0091-7613(1987)15<549:ITORFA>2.0.CO;2.
- Swanson, S.E., 1977, Relation of nucleation and crystal-growth rate to the development of granitic textures: *The American Mineralogist*, v. 62, p. 966–978.
- Tuffen, H., and Castro, J.M., 2009, The emplacement of an obsidian dyke through thin ice: Hrafninnuhryggur, Krafla Iceland: *Journal of Volcanology and Geothermal Research*, v. 185, p. 352–366, doi:10.1016/j.jvolgeores.2008.10.021.
- Tuffen, H., James, M.R., Castro, J.M., and Schipper, C.I., 2013, Exceptional mobility of an advancing rhyolitic obsidian flow at Cordón Caulle volcano in Chile: *Nature Communications*, v. 4, 2709, doi:10.1038/ncomms3709.
- Vazquez, J.A., Kyriazis, S.F., Reid, M.R., Sehler, R.C., and Ramos, F.C., 2009, Thermochemical evolution of young rhyolites at Yellowstone: Evidence for a cooling but periodically replenished post-caldera magma reservoir: *Journal of Volcanology and Geothermal Research*, v. 188, p. 186–196, doi:10.1016/j.jvolgeores.2008.11.030.
- von Aulock, F.W., Nichols, A.R.L., Kennedy, B.M., and Oze, C., 2013, Timescales of texture development in a cooling lava dome: *Geochimica et Cosmochimica Acta*, v. 114, p. 72–80, doi:10.1016/j.gca.2013.03.012.
- Walker, G.P.L., Huntington, A.T., Sanders, A.T., and Dinsdale, J.L., 1973, Lengths of lava flows [and discussion]: *Philosophical Transactions of the Royal Society of London*, v. 274, p. 107–118, doi:10.1098/rsta.1973.0030.
- Watkins, J., Manga, M., Huber, C., and Martin, M., 2009, Diffusion-controlled spherulite growth in obsidian inferred from H₂O concentration profiles: *Contributions to Mineralogy and Petrology*, v. 157, p. 163–172, doi:10.1007/s00410-008-0327-8.

Manuscript received 22 January 2015

Revised manuscript received 12 May 2015

Manuscript accepted 13 May 2015

Printed in USA